

Aircraft Identification by Unions of ISAR Images

Vesna Zeljkovic
AMTP Department
Delaware State University
Dover, DE 19901 USA
1 302 3998962

vzeljkovic@comcast.net

Claude Tameze
AMTP Department
Delaware State University
Dover, DE 19901 USA

Qiang Li
AMTP Department
Delaware State University
Dover, DE 19901 USA

Fengshan Liu
AMTP Department
Delaware State University
Dover, DE 19901 USA

Robert B. Vincelette
AMTP Department
Delaware State University
Dover, DE 19901 USA

ABSTRACT

We offer an algorithm that can identify aircraft categories from Inverse Synthetic Aperture Radar (ISAR) images that use both the radar reflection pulse shape, which includes the duration or size of the radar pulse that is reflected, and the Doppler shifts of different parts of the aircraft caused by rotational motions of the aircraft as it maneuvers. We investigated the practicality of determining which of seven different aircraft categories a radar return indicates. The object of this research is to very quickly tell from an ISAR return how an aircraft compares to the seven different categories where the aircraft is in any position of a prescribed holding pattern. We propose a new method in which we compare each ISAR image to unions of images of the different aircraft categories. This method gave us results that are superior to the results we obtained in [8].

Keywords

ISAR images, classification, pattern recognition.

1. INTRODUCTION

In military applications, it is desirable to be able to automatically identify the aircraft model from as little radar information as possible. It is likely that the combat crews of attacking aircraft will do everything they can to deprive their target of the use of radar information about their attack. Usually, automatic electronic countermeasure avionics on the attacking aircraft or an electronics warfare officer in the flight crew will jam the radar as soon as the radar is detected. The target of the attack will have only the first radar pulses to try to identify what categories of aircraft are making the attack. It would be a great advantage to know from as little as one returned radar pulse what kind of aircraft are involved. Many methods of ISAR target recognition have been developed. [1]-[4] test only features taken from the ISAR image.

Permission to make digital or hard copies of all or part of this work for personal or classroom use is granted without fee provided that copies are not made or distributed for profit or commercial advantage and that copies bear this notice and the full citation on the first page. To copy otherwise, or republish, to post on servers or to redistribute to lists, requires prior specific permission and/or a fee. Mobimedia'09, September 7-9, 2009, London, UK. Copyright 2009 ICST 978-963-9799-62-2/00/0004 ... \$5.00

This is faster than trying to compare the whole target aircraft. Some methods [5]-[7] use optimal classifiers.

Section 2 of this paper gives the mathematical formulation of ISAR image construction and explains the difficulties in its construction. Section 3 gives the details of the proposed ISAR image classification. Section 4 gives our experimental results and compares them to our previous method we described in [8] and Section 5 gives our conclusions.

2. ISAR IMAGE CONSTRUCTION

ISAR images are constructed by processing a radar reflection from a moving target and the Doppler shifts caused by rotational motions of the target. Figure 1 shows the geometry of the radar target, the radar station, and the Doppler shifts caused by relative motions of parts of the aircraft as rotational maneuvers take place. The target is rotating about an origin, O, of an X-Y Cartesian coordinate system. The origin is a distance r_a from the radar. Any point, P, on the target has coordinates, r_o , θ_o from O.

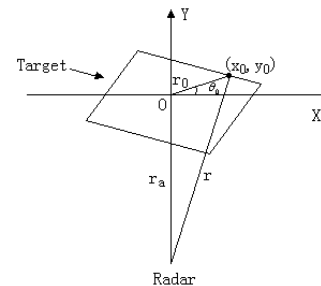


Figure 1. Variant cross-range scale.

The target is rotating about O with an angular velocity of ω . The distance from the radar to point P(r_o , θ_o) at time t will be

$$r(t) = [r_o^2 + r_a^2 + 2r_o r_a \sin(\theta_o + \omega t)]^{1/2} \quad (1)$$

But radar targets are far field, that is, $r_a \gg r_o$, so equation (1) can be approximated:

$$r(t) \approx r_a + x_o \sin \omega t + y_o \cos \omega t \quad (2)$$

Rotation will introduce a Doppler shift.

$$f_d = \frac{2}{\lambda} \frac{d}{dt} r(t) = \frac{2x_0\omega}{\lambda} \cos \omega t - \frac{2y_0\omega}{\lambda} \sin \omega t \quad (3)$$

λ is the wavelength of the radar. We make a further approximation that t is a very small time after t_0 .

$$r = r_a + y_0 \quad (4)$$

$$f_d = 2x_0\omega/\lambda \quad (5)$$

From equation (4) we determine the y_0 coordinate and from equation (5) we determine a corresponding x_0 coordinate that is proportional to f_d divided by the unknown value of ω . This makes it possible to construct an image from all points $P(x_0, y_0)$ that is fixed in the vertical scale of the Y axis and variable in the horizontal scale of the X axis. This image gives us useful information about the shape of the aircraft, [9]-[10].

ISAR imaging gives an image of a target from range and Doppler shifts caused by rotation of the aircraft. If there is sufficient Doppler shift sampling frequency and observation window, the image can be easily recognized by ISAR or human perception. However, there are limits of what it can see. These limits are due to Doppler induced distortion and reflection characteristics and shadows.

Doppler frequency shifts vary with the direction and speed of the rotation vector ω . The radar return also changes with the rotational position, θ . Rotating parts on aircraft, such as propeller blades or rotating compressor blades of jet engines introduce Doppler modulations.

When the incident electromagnetic radiation of a radar pulse encounters an aircraft it is subjected to the laws of optics. It can be scattered by passage through boundaries between media of different dielectric constants, it can be reflected, or it can be absorbed. The sheet aluminum skin of many aircraft (typically 2024 T3 alloy) is a very efficient reflector at radar frequencies. These reflections are influenced by several things, including the cross sectional area the aircraft presents to the radar receiver antenna. A long thin aircraft with a heading parallel to the Pointing vector of the radar will make a smaller echo than an aircraft illuminated broadside because the former orientation offers a smaller cross sectional area than the latter. The shape of the reflecting surface has a great effect on how much radar is reflected back to the radar receiving antenna. Edge diffraction is significant at radar frequencies. Also, like any other form of illumination, parts of the aircraft will cast shadows that will make other parts of the aircraft invisible to the radar receiver.

3. ISAR IMAGE CLASSIFICATION

The proposed algorithm for ISAR image classification is very simple. It makes a single comparison of one ISAR image to the union of images of all positions of the aircraft category in a holding pattern. This new method produced results that are superior to the results we obtained in [8]. We have in memory 360 different ISAR images of aircraft categories 1 through 5, 180 different ISAR images for category 6 and 60 images for category 7. These ISAR images represent different positions of aircraft in

their holding patterns. The procedure of the ISAR image classification algorithm is the following:

- 1) For each category, we take the center of gravity of each ISAR image. We do this because when we compare one image to another, we place one over the other and find how many pixels of one image intersect those of the other image. This is usually a maximum number when the images are positioned with their centers of gravity concurrent
- 2) We form ISAR images union in which all centers of gravity are concurrent.

$$R(x, y) = \bigcup_{i=1}^N I_i(x, y) \quad (6)$$

where N is the number of ISAR images in the holding pattern and $R(x, y)$ is the pixel in the formed union image. $I_i(x, y)$ is the set of pixels of each ISAR image that belongs to the airplane in the data base for each aircraft category.

- 3) We compare the analyzed object with the shapes from the database by placing it over each of the seven category unions, $R(x, y)$.

- 4) We calculate the similarity coefficient between the ISAR return and each of the category unions based on the following formula:

$$sim = 1 - \arccos \left[\frac{I_1^T * I_2}{norm(I_1) * norm(I_2)} \right] \quad (7)$$

- 5) The category that gives the largest similarity coefficient with the analyzed object is considered the most likely match.

4. ISAR IMAGE SIMULATIONS

We simulate the ISAR images of seven different categories of aircraft flying a left hand holding pattern as depicted in Figure 5. The positions of the simulated flight in the holding pattern do not always correspond to aircraft heading but rather to evenly spaced positions in the holding pattern.

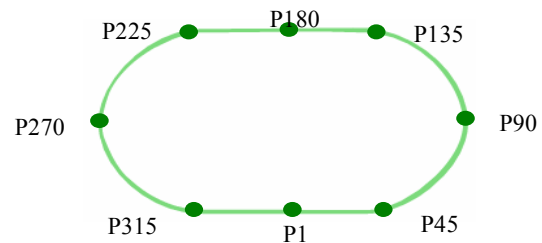


Figure 5. Target Trace Point Position (Top View).

We are comparing six different artificially simulated categories of airplanes and one real aircraft category that has a lot of noise present in the ISAR images. The seven tested aircraft categories are presented in Figure 6. The first five categories have 360 different rotational orientations from which ISAR images are taken throughout the holding pattern. Category 6 has half the resolution of the first five categories, that is, it has only 180 different ISAR images. Category 7 has only 60 ISAR images. We simulated the categories 1 to 5. Categories 6 and 7 are taken from Internet.

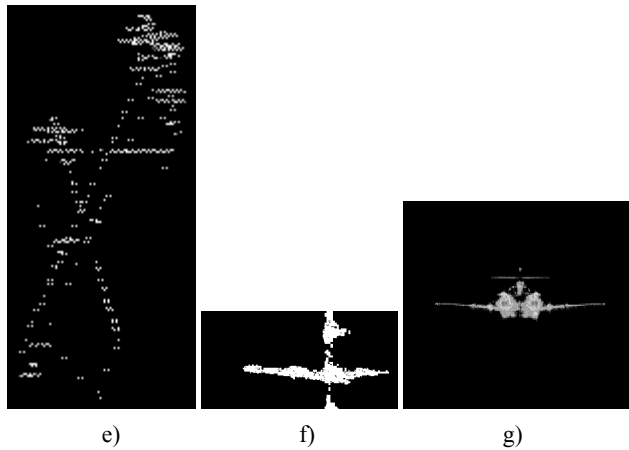
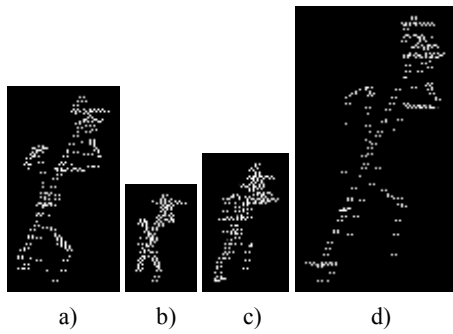


Figure 6. Classified airplane models: a) Category 1; b) Category 2; c) Category 3; d) Category 4; e) Category 5; f) Category 6; g) Category 7.

We take every picture from the database for the comparison which consists of the images that represent all 360, 180 and 60 different positions in the paths of all seven different airplane models. We test for what parts of the holding pattern it is possible to automatically identify what kind of aircraft corresponds to the ISAR image. We compare the unknown model with the union images of every aircraft category present in the database that are shown in Figure 7.

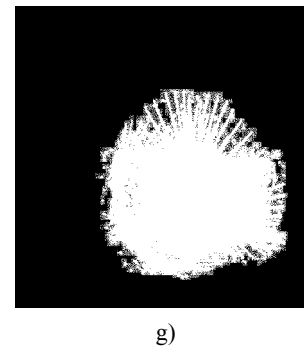
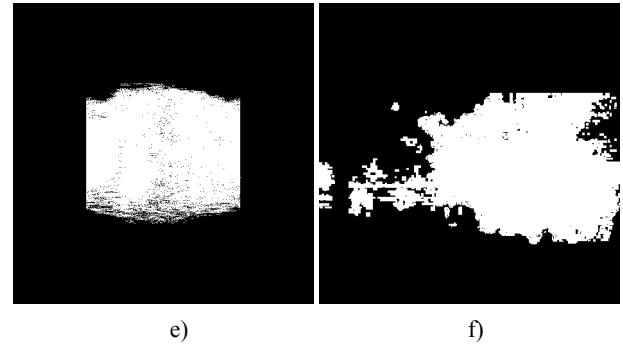
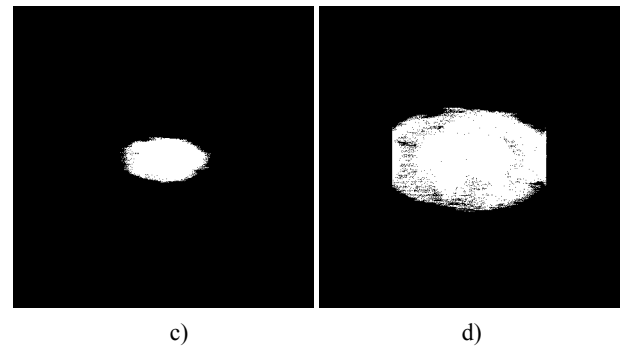
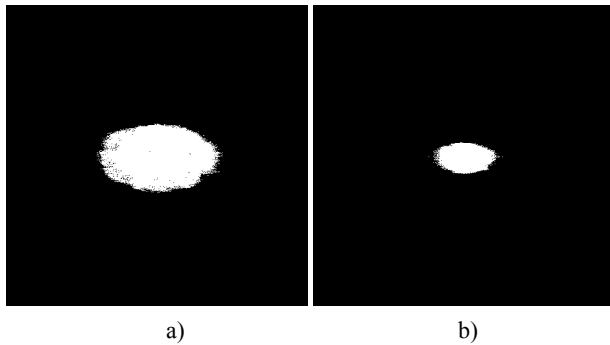


Figure 7. Union image of airplane models: a) Category 1; b) Category 2; c) Category 3; d) Category 4; e) Category 5; f) Category 6; g) Category 7.

We took each individual image, all 360 of them from categories 1 through 5, 180 from category 6 and 60 from category 7, and tested it according to the proposed classification algorithm.

The category that yielded the highest similarity coefficient was what we considered a match. Table 1 shows the results of the proposed method for automated aircraft model classification.

- A - Airplane Category**
- B - Number of images in holding pattern**
- C - Misclassified positions**
- D - Category misclassified**
- E - Number of misclassifications**
- F - Percent of misclassifications**

Table 1. Summary of the obtained results

A	B	C	D	E	F
1	360	112, 125, 128	3	3	0.83 %
2	360	-	-	0	0 %
3	360	101, 103, 105, 116-122, 125-129, 131-136, 141,142, 145-147, 151, 153, 155	2	28	7.78 %
4	360	117-122, 125, 126	1	8	2.22 %
5	360	115	4	1	0.28 %
6	180	-	-	0	0 %
7	60	-	-	0	0 %

Table 2. Summary of the obtained results in [8]

A	B	C	E	F
1	360	100,120,140,180 280,300,320,340	8	26.67 %
2	360	280,300,340	3	10 %
3	360	80,120, 280,300, 320, 340, 360	7	23.33 %
4	360	100,120,180,200 260,280,300,320 340,360	10	33.33 %
5	360	100,120,140,160	4	13.33 %
6	180	60, 180	2	22.22 %
7	60	-	0	0 %

The obtained results show that the algorithm fails to correctly classify the observed airplane mostly on the right upper curved part of the airplane paths which means in the positions 112°, 125° and 128° for the first airplane category, in the positions from 101° to 155° for the third category, in the positions from 117° to 122°, 125° and 126° for the fourth category and in the position from 115° for the fifth category. In these positions the aircraft was rolling into a left turn. The images of these positions that are incorrectly classified by the algorithm are marked in the Table 1. These positions are even visually critical ones for the recognition. This is the part of the holding pattern when the aircraft fly towards the radar. In these positions the wings become nearly invisible and the wings and the nose of the airframe present a small radar cross section area because the aircraft is heading almost directly towards the radar station. This could be affected by the thickness and size of the wings and how airfoil curvature scatters the incident radiation. Figures 8-11 show the images of the critical positions for all airplane models that are even visually difficult to distinguish.

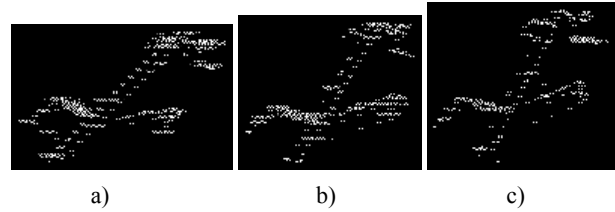


Figure 8. Category 1 at misclassified positions: a) 112; b) 125; c) 128.



Figure 9. Category 3 at misclassified positions: a) 105; b) 120; c) 125; d) 135; e) 155.

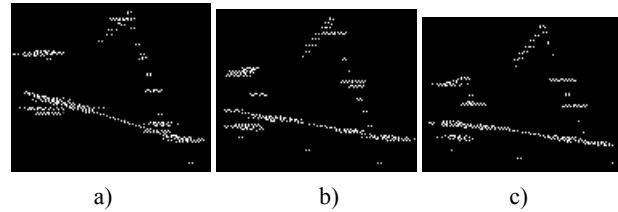


Figure 10. Category 4 at misclassified positions: a) 120; b) 125; c) 126.



Figure 11. Category 5 at misclassified position 115.

As Table 1 summarizes, category 2, 6 and 7 suffered no misclassifications. Categories 1 and 5 have less than 1% misclassifications and only one as high as 7.78 %. What is surprising is that categories 6 and 7, which have less information because they have only 180 and 60 images respectively had no misclassifications. Category 6 contains significant noise which makes the classification more difficult. The proposed automated algorithm has shown itself to be resistant to the severe noise present.

The ISAR imaging environment varies and it is difficult to make comparison of different airplane identification methods on various aircraft models. The results obtained with the proposed classification method are compared to the results shown in Table 2 obtained using the method described in [8] on the same aircraft

model sets. This method shows itself to be much more successful in correct and efficient classification than the one described in [8]. The percent of correctly classified images with the proposed method is three to thirty times higher than with the method proposed in [8].

5. CONCLUSION

During most of the holding pattern, our new method that uses unions of images successfully identified the category to which each ISAR image belonged. Categories 2, 6, and 7 had no errors and Category 3 showed the largest identification error of less than 8%. Category 4 had approximately 2.2% error, Category 1 had less than 1% error and Category 5 had less than 1/3 % error.

These results are remarkable considering the limits of what information radar can convey in the reflection off an aircraft. During the parts of the flights, when the program failed to identify aircraft category, large portions of the aircraft disappear from the ISAR images which is normal in the holding pattern. These ISAR images were even visually difficult to distinguish by human interaction.

The proposed algorithm is far superior in both speed and accuracy to the results obtained in our earlier work [8].

For future research we hope to be able to flight test several aircraft against an ISAR equipped radar in the field. Smaller aircraft are affordable to rent for this purpose.

6. ACKNOWLEDGMENTS

This work is partially supported by DoD HBCU/MI Infrastructure Support Program (45395-MA-ISP Department of Army) and partially supported by the US Army Research Office under contract P-54412-CI-ISP. Special thanks to Ruzica Vlajkovic and Milos Zeljkovic.

7. REFERENCES

- [1] Saidi, M.N.; Hoeltzner, B. et al., "Recognition of ISAR Images: Target Shapes Features Extraction", ICTTA 2008 3rd International Conference, Vol:7-11, April 2008, pp.1-6.
- [2] Maskall, G.T. "An application of nonlinear feature extraction to the classification of ISAR images", RADAR 2002, Vol.15-17, October 2002 pp: 405 - 408.
- [3] Vespe M., Baker C.J., Griffiths H.D., "Outline Structural Representation for Radar Target Classification Based on Non-Radar Templates", Radar 2006, CIE '06 International Conference on 16-19 October 2006, pp. 1-4.
- [4] Manikandan, J., Venkataramani, B., Jayachandran, M., "Evaluation of Edge Detection Techniques towards Implementation of Automatic Target Recognition", Conference on Computational Intelligence and Multimedia Applications 2007, International Conference on Volume 2, 13-15 December 2007, pp. 441-445.
- [5] Kyung-Tae Kim, Dong-Kyu Seo, Hyo-Tae Kim, "Efficient classification of ISAR images", Antennas and Propagation, IEEE Transactions, Vol. 53-5, May 2005, pp. 1611-1621.
- [6] Martorella, M., Giusti E. et al., "Automatic Target Recognition by means of polarimetric ISAR images: a model matching based algorithm", Radar 2008 International Conference on 2-5 September 2008, pp. 27-31.
- [7] H. Yuankui, Y. Yiming, "Automatic target recognition of ISAR images based on Hausdorff distance", APSAR 2007, 5-9 November 2007, pp. 477-479.
- [8] V. Zeljković, Q. Li, R. Vincelette, C. Tameze, F. Liu, "Automatic Algorithm for ISAR Images Recognition and Classification", Signal and Data Processing of Small Targets 2009 conference.
- [9] Prickett, M. J.; Chen, C. C., Principles of inverse synthetic aperture radar imaging, In: EASCON '80; Electronics and Aerospace Systems Conference, Arlington, VA, September 29-October 1, 1980, Conference Record. (A81-48526 24-32) New York, Institute of Electrical and Electronics Engineers, 1980, p. 340-345.
- [10] Qiang Li, Study of Monopulse Radar Target Three Dimensional Imaging and Recognition, Ph.D dissertation. Xidian University, 2007, p.33